Current-Mode Integrator using OA and OTAs and Its Applications

Katesuda Klahan, Worapong Tangsrirat, Wanlop Surakampontorn
Faculty of Engineering , King Mongkut's Institute of Technology Ladkrabang (KMITL),
Ladkrabang, Bangkok 10520, Thailand

Teerasilapa Dumawipata
Department of Industrial Electrical Technology (IET), Faculty of Engineering,
King Mongkut's Institute of Technology North-Bangkok (KMITNB),
Bangsue, Bangkok 10800, Thailand

Abstract

A circuit building block for realizing a continuous-time active-only current-mode integrator is presented. The proposed integrator is composed only of an internally compensated type operational amplifier (OA) and operational transconductance amplifiers (OTAs). The integrator is suitable for integrated circuit implementation in either bipolar or CMOS technologies, since it does not require any external passive elements. Moreover, the integrator gain can be tuned through the transconductance gains of the OTAs. Some application examples in the realization of current-mode network functions using the proposed current-mode integrator as an active element are also given.

Keywords: current-mode integrator, driving-point impedance functions , current-mode filters

1. Introduction

In the last decade, the realizations of various active circuits by utilizing the operational amplifier (OA) pole have received considerable attention for their potential advantages, such as being attractive for monolithic IC integration, ease to design, and suitability for high frequency operation [1-2]. Several OA-based active-R capacitor-less circuits for realizing analog transfer functions have been reported [3-4]. Presently, there is a strong motivation to design resistor-less and capacitor-less filter circuits utilizing the finite and complex gain natures of internally compensated OAs and OTAs. Due to its active only nature, the resistor-less and capacitor-less active filter would be attractive for its programmability and wide frequency range of operation. Many implementations of active-only filter designs are available in the literature [5-7].

An integrator is an important circuit building block, which is widely used in analog signal processing applications, such as, filter design, waveform shaping, process controller design, and calibration circuits, etc. However, the implementation of a continuous-time current-mode integrator that employs only active elements has not yet been reported. Therefore, a circuit configuration for realizing active-only current-mode integrator is proposed in this paper. The proposed integrator consists of one OA and two OTAs. Moreover, it can be implemented in integrated circuit form in both bipolar and CMOS technologies. The integrator gain can be electronically tuned by adjusting the transconductance gains of the OTAs. Various accomplishment active-only analog signal processing circuits employing the proposed integrator will also be presented. Finally, the workabilities of the proposed integrator and its applications have been simulated based upon an LM741 type IC OA and a CA3080 type IC OTA.

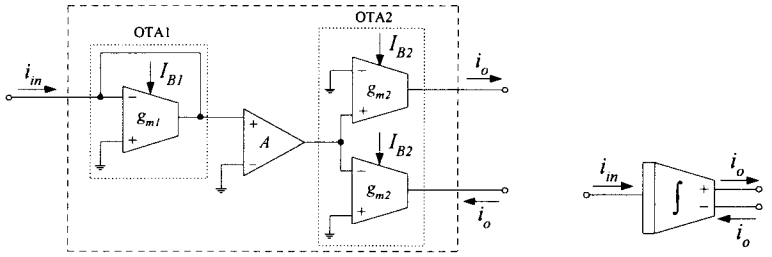

(a) (b)

Fig. 1 : The proposed active-only current-mode integrator
(a) circuit implementation (b) circuit representation

2. Circuit Description

The proposed active-only dual-output current-mode integrator and its representation are shown in Fig. 1. The integrator consists only of an OA and OTAs, where the dual-output-currents are implemented by using single-ended output OTAs in parallel connection [8]. If ω_a is the 3-dB bandwidth of the OA and by considering the OA for the frequencies $\omega >> \omega_a$, the open-loop gain $A_{OA}(s)$ of the OA can be approximately given by

$$A_{OA}(s) = \frac{A_O \omega_a}{s+\omega_a} \cong \frac{B}{s} \qquad (1)$$

where B represents the gain-bandwidth product (GBP) of the OA, which is the product of the dc gain A_o and the 3-dB bandwidth ω_a, assuming that g_{m1} and g_{m2} denote the transconductance gains of the OTA1 and OTA2, respectively. Then the current transfer function of the current-mode integrator can be expressed as:

$$\frac{I_O(s)}{I_{in}(s)} = \frac{B}{s}\left[\frac{g_{m2}}{g_{m1}}\right] = \frac{B}{s} A_G \qquad (2)$$

where A_G is the ratio between g_{m2} and g_{m1} and denotes the integrator gain. Eqn. (2) indicates that the relationship of the currents I_o and I_{in} is in the form of the integrating action. It should be noted that for ordinary bipolar OTAs, $g_{m1} = I_{B1}/2V_T$ and $g_{m2} = I_{B2}/2V_T$, where V_T is the thermal voltage and I_{B1} and I_{B2} are the bias currents of the OTA1 and OTA2, respectively. Thus, eqn. (2) becomes

$$\frac{I_o(s)}{I_{in}(s)} = \frac{B}{s}\left[\frac{I_{B2}}{I_{B1}}\right] = \frac{B}{s} A_G \qquad (3)$$

A_G is the current gain, that is the current ratio between the bias current I_{B2} and I_{B1}. In this case, the temperature dependence of the transconductance gains g_{m1} and g_{m2} of the bipolar OTAs are compensated.

Deviation from the ideal performance predicted from eqn.(2) is due to parasitic effects of the non-ideality characteristics of the OA and OTAs. If the second dominant pole ω_b of the OA is taken for consideration, the OA open-loop gain $A_{OA}(s)$ can be rewritten as

$$A_{OA}(s) = \frac{B}{s}\frac{\omega_b}{(s+\omega_b)} = \frac{B}{s}\frac{1}{(1+\tau_b s)} \qquad (4)$$

where $\tau_b = 1/\omega_b$. For the OTAs, let $\omega_c = 1/\tau_c$ represent the effective transconductance internal-pole of the OTA and g_{m0} is the low frequency transconductance gain. The OTA open-loop gain $g_m(s)$ for the general case can be described by

$$g_m(s) = \frac{g_{m0}}{\left(1+ s/\omega_c\right)} \cong g_{m0}\left(1- s/\omega_c\right) \qquad (5)$$

Therefore, the frequency response of the current-mode integrator in Fig. 1 (including the second dominant pole of the OA) and the transconductance internal-poles of the OTAs can now be given by

$$\frac{I_o(s)}{I_{in}(s)} = \left[\frac{B}{s}\right]\left[\frac{1}{1+\tau_b s}\right]\left[\frac{g_{m02}}{g_{m01}}\right]\left[\frac{\omega_{c2}-s}{\omega_{c2}}\right]\left[\frac{\omega_{c1}}{\omega_{c1}-s}\right] \qquad (6)$$

where ω_{c1} and ω_{c2} are the effective transconductance internal-poles of OTA1 and OTA2, respectively. It can be seen that if the conditions $\omega_{c1} \cong \omega_{c2}$ and $\omega_{c1} >> \omega$, $\omega_{c2} >> \omega$ are

satisfied, then eqn. (6) becomes frequency independent. As a result, if we define $A_{G0} = g_{m02}/g_{m01}$, eqn. (6) can be reasonably reduced to

$$\frac{I_O(s)}{I_{in}(s)} = \left[\frac{A_{G0}B}{s}\right]\left[\frac{1}{1+\tau_b s}\right] \qquad (7)$$

One can see that the frequency characteristic of the proposed current-mode integrator has a dc current gain equal to eqn. (2) and a high frequency dominant pole located at ω_b. Hence, the OA pole ω_b should be the major high-frequency limitation of the proposed current-mode integrator. For example, the commercially available LF356N OA has the gain-bandwidth product $B = 2\pi(4.5)\times10^6$ rad/s and its second dominant pole is $\omega_b = 2\pi(9)\times10^6$ rad/s [9]. Hence, the major high-frequency limitation of the proposed integrator is approximately located at 9 MHz.

3. Application Examples

The following sections will concentrate on the usefulness of the proposed current-mode integrator. Some application examples to realize driving-point impedance functions and current-mode biquadratic filters will be considered.

3.1. Driving-point impedance functions

3.1.1. Inductance simulations

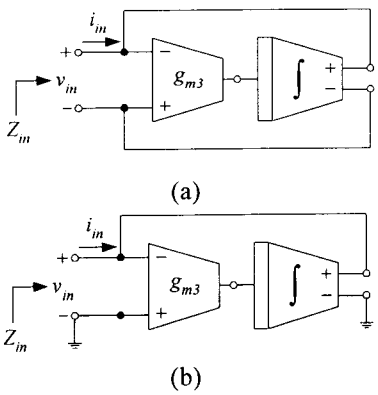

Fig. 2 : Active-only inductance simulations

Fig. 2(a) and Fig. 2(b) show the circuit diagram of a tunable floating and a grounded inductance simulations, respectively. From the circuits, it can easily be shown that the value of the simulated inductance is

$$L_{eq} = \left[\frac{1}{g_{m3}A_G B}\right] \qquad (8)$$

It should be noted that the equivalent inductance L_{eq} can properly be tuned by electronic means through the current ratio A_G and/or the transconductance gain g_{m3}.

3.1.2. Capacitance simulations

An application of the proposed current-mode integrator to simulate an electronically tunable capacitance simulation circuit is shown in Fig.3. In this case, the magnitude of the simulated capacitance can be given by

$$C_{eq} = \left[\frac{g_{m4}g_{m5}}{g_{m3}A_G B}\right] \qquad (9)$$

Since A_G and g_{mi} (i = 3, 4, 5) can be electronically variable, the magnitude of the simulated capacitance can also be electronically variable. In the same manner, the grounded capacitance multiplier of Fig. 3 can be conveniently converted into a corresponding floating capacitance by adding an additional dual-current output OTA.

3.1.3. Frequency-dependent negative resistance (FDNR)

The scheme for simulating a frequency-dependent negative resistance (FDNR) element is shown in Fig. 4. Also, note that the circuit behaves as a grounded FDNR element with

$$D = \left[\frac{g_{m6}g_{m7}}{g_{m5}A_{G1}A_{G2}B_1B_2}\right] \qquad (10)$$

where A_{Gi} and B_i are the gain and the OA's GBP of the i-th integrator unit (i = 1, 2). In contrast to conventional circuits, this circuit does not require any external passive elements and its characteristic can be electronically tuned.

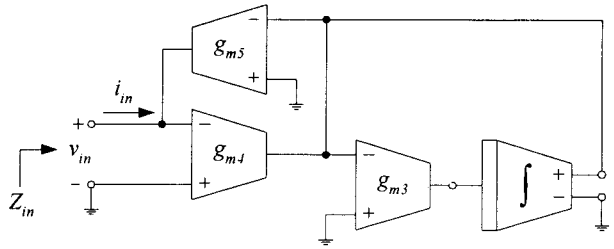

Fig. 3 : Grounded-capacitance multiplier simulation

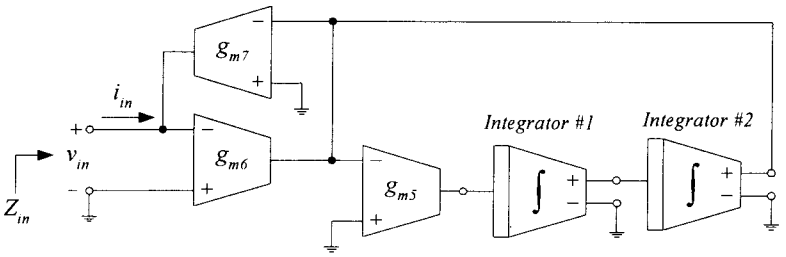

Fig. 4 : An active-only FDNR

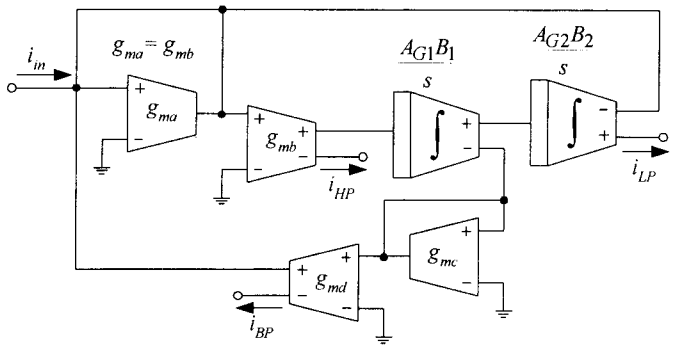

Fig. 5 : Active-only current-mode biquadratic filter

3.2. Electronically tunable active-only current-mode biquadratic filter

Fig. 5 shows the circuit diagram of the tunable current-mode filter based on the proposed current-mode integrator, where i_{LP} , i_{BP}, and i_{HP} are the lowpass, bandpass and highpass current-output terminals, respectively. The circuit parameters ω_o and Q-factor of this filter can be written as

$$\omega_O = \sqrt{A_{G1}A_{G2}B_1B_2} \qquad (11)$$

and

$$Q = \frac{g_{mc}}{g_{md}}\sqrt{\frac{A_{G2}B_2}{A_{G1}B_1}} \qquad (12)$$

One can see that the filter also enjoys orthogonal tuning of ω_o and Q-factor via the transconductance gains of the OTAs and it is also temperature independent.

To discuss the non-ideal effect of the proposed integrator on the filter's frequency characteristics, the parasitic second dominant pole of the OA from equation (7) is taken into account. As a result, the percentage inaccuracies of the ω_o and Q-factor in this case are respectively found to be

$$\frac{\delta\omega_o}{\omega_o} = \left\{\left[1+\left(A_{G1}B_1\tau_{b1}\right)\left(A_{G2}B_2\tau_{b2}-\frac{g_{md}}{g_{mc}}\right)\right]^{1/2}-1\right\}\times 100\% \qquad (13)$$

and

$$\frac{\delta Q}{Q} = \frac{\left[1-\left(\frac{g_{mc}A_{G2}B_2}{g_{md}}\right)\left(\tau_{b1}+\tau_{b2}\right)\right]-\left[1+\left(A_{G1}B_1\tau_{b1}\right)\left(A_{G2}B_2\tau_{b2}-\frac{g_{md}}{g_{mc}}\right)\right]^{1/2}}{\left[1+\left(A_{G1}B_1\tau_{b1}\right)\left(A_{G2}B_2\tau_{b2}-\frac{g_{md}}{g_{mc}}\right)\right]^{1/2}}\times 100\% \qquad (14)$$

where $\omega_{b1} = 1/\tau_{b1}$, $\omega_{b2} = 1/\tau_{b2}$ and ω_{b1} and ω_{b2} are the second dominant poles of the OA1 and OA2, respectively. It is found that undesirable factors, which are yielded by the parasitic effects of OAs, can be made negligible if such factors are considered as the condition:

$$1 >> \left(\frac{g_{mc}A_{G2}B_2}{g_{md}}\right)\left(\tau_{b1}+\tau_{b2}\right) \qquad (15)$$

4. Design Examples And Simulation Results

In order to verify the theoretical study of the proposed current-mode integrator, PSPICE simulation results are included. In this simulation, the OTA is modeled by employing a CA3080 type OTA with a macro model [8] and an LM741 type OA with the gain-bandwidth product $B = 2\pi\times10^6$ rad/s. Fig. 6 shows the simulated frequency responses of the proposed current-mode integrator. The results show that the circuit acts as an integrating function with a slope -20 dB per decade for the frequency range from 10 Hz to 1 MHz and has less than 10% phase error in the frequency range of 30 Hz to 500 kHz.

The performance of the floating inductance circuit of Fig. 2(a) is demonstrated through the use of an electronically tunable active RL low-pass filter in Fig. 7(a) with the external resistor R_1 = 1 kΩ. The bias current ratio $A_G = I_{B2}/I_{B1}$ (= g_{m2}/g_{m1}) is set to 0.5, 1 and 2, while g_{m1} and g_{m3} are respectively set to 1 mS and 0.4 mS ; thus the cut-off frequencies f_C are approximately equal to 200 kHz, 400 kHz and 800 kHz, respectively. The frequency responses of the low-pass filter are shown in Fig. 7(b).

Fig. 8 shows simulated responses of the tunable current-mode multifunctional filter of Fig. 5, when $A_{G1} = A_{G2} = 0.05$ and $g_{mc}/g_{md} = 0.1$. This filter is designed for $\omega_o/2\pi$ = 50 kHz at the unity Q-factor. All the simulated results shown above imply that the proposed integrator exhibits reasonably good agreement with the predicted values.

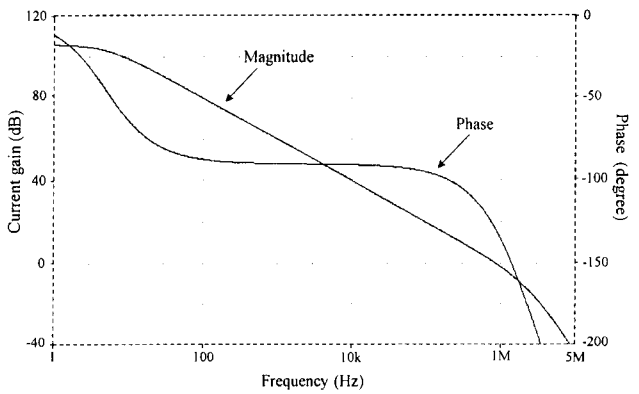

Fig. 6 : Frequency responses of the proposed integrator

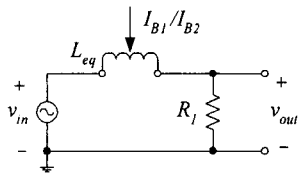

(a)

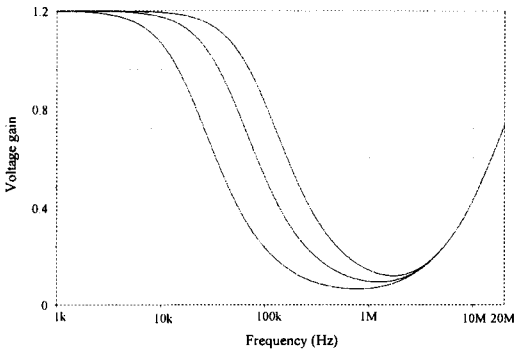

(b)

Fig. 7 : (a) first-order RL lowpass filter
(b) frequency responses of the simulated RL lowpass filter

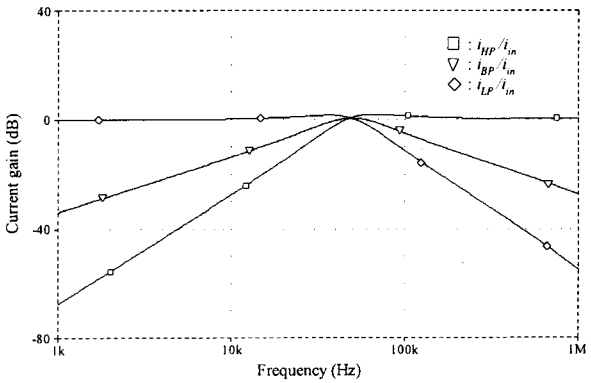

Fig. 8 : Simulated frequency response of current-mode filter of Fig. 5

5. Conclusions

This paper presented an alternative scheme for realizing a continuous-time active-only current-mode integrator. The proposed integrator is realized using only internally compensated type OA and OTAs, and does not require any external passive elements. Because of its active-only nature, the integrator can be easily employed to realize active network functions and are suitable for implementing in monolithic integrated form in both bipolar or CMOS technologies. Since the proposed circuit utilizes an OA pole, it is also suitable for high frequency operation. The simulated results have been used to verify the theoretical analysis.

6. Acknowledgment

This work is partly funded by the Thailand Research Fund (TRF) under the Senior Research Scholar Program, grant number RTA/04/2543. The support provided by the Japan International Cooperation Agency (JICA) is also acknowledged.

7. References

[1] Brand, J.R. and Schaumann, R., Active-R Filters: Review of Theory and Practice, Electronic Circuits and Systems, Vol. 2, pp. 89-101, 1978.

[2] Kumar, U. and Shukla, S.K., On the Importance, Realization, Experimental Verification and Measurement of Active-R and Active-C Filters, Microelectronics J., Vol. 21, pp. 21-45, 1990.

[3] Higashimura, M., Current-mode Lowpass and Bandpass Filters Using the Operational Amplifier Pole, Int. J. Electron., Vol. 74, pp. 945-949 , 1993.

[4] Soderstrand, M.A., Watt, V.H.C., Kee , K.B. and Mcginity, D., Implementation of an Active-R Filter Building Block in Semi-Custom VLSI, Int. J. Electron., Vol. 76, pp. 469-482, 1994.

[5] Singh, A.K. and Senani, R., Low-component-count Active-only Imittances and their Application in Realizing Simple Multifunction Biquads, Electron. Lett., Vol. 34, pp. 718-719, 1998.

[6] Abuelma'atti, M.T. and Alzaher, H.A., Universal three Inputs and One Output Current-Mode Filter Without External Passive Elements, Electron. Lett., Vol. 33, pp. 281-283, 1997.

[7] Tsukutani, T., Higashimura, M., Sumi, Y. and Fukui, Y., Electronically Tunable Current-Mode Active-Only Biquadratic Filter, Int. J. Electron., Vol. 87, pp. 307-314, 2000.

[8] Wu, J., Current-Mode High-Order OTA-C Filters, Int. J. Electron., Vol. 76, pp. 1115-1120, 1994.

[9] Bowron, P., O'Carroll, A.P. and Daaboul, A.A., Polynomial Reduction in the Analysis of Active-Filter Parasitics, IEEE Trans. on Circuits and Systems, Vol. 36, pp. 1020-1023, 1989.